

SUPPLEMENTAL FIGURE LEGENDS

FIGURE S1. CTA1₁₋₁₆₈ does not bind to plasma membrane or lipid raft LUVs. The affinity between CTA1₁₋₁₆₈ and the plasma membrane (A, C, E) or lipid rafts (B, D, F) was determined by tryptophan RET using pyrene-labeled LUVs (A, B) or unlabeled LUVs (C, D). For the representative spectra in panels A-D, a change of color from blue to red signifies an increase in lipid concentration from 100 to 1000 μ M. Each measurement of fluorescent intensity for both labeled and unlabeled LUVs was normalized to the CTA1 concentration at the start of the experiment (i.e., corrections were made for the sample dilution effect). Curve fitting of the data is presented in panels E & F.

FIGURE S2. CTA1₁₋₁₆₈ is not stabilized by plasma membrane or lipid raft LUVs. The temperature-induced unfolding of CTA1₁₋₁₆₈ in the presence of plasma membrane (A-C) or lipid raft (D-F) LUVs was recorded by far-UV CD (A, D), near-UV CD (B, E), and fluorescence spectroscopy (C, F). The change in color from blue to red denotes the increase in temperature from 20°C to 60°C. (G-I) Thermal unfolding profiles for CTA1₁₋₁₆₈ in the presence of plasma membrane (green) or lipid raft (blue) LUVs were derived from the data presented in panels A-F. (G) For far-UV CD analysis, the mean residue molar ellipticities at 220 nm ($[\theta]_{220}$) were plotted as a function of temperature. (H) For near-UV CD analysis, the mean residue molar ellipticities at 280 nm ($[\theta]_{280}$) were plotted as a function of temperature. (I) For fluorescence spectroscopy, the maximum emission wavelength (λ_{\max}) was plotted as a function of temperature.

FIGURE S3. Stabilization of CTA1 by sphingomyelin-depleted lipid raft LUVs. The temperature-induced unfolding of CTA1 in the presence of sphingomyelin-depleted lipid raft LUVs was recorded by far-UV CD (A), near-UV CD (B), and fluorescence spectroscopy (C). The change in color from blue to red denotes the increase in temperature from 20°C to 60°C. (D) For far-UV CD analysis, the mean residue molar ellipticities at 220 nm ($[\theta]_{220}$) were plotted as a function of temperature. (E) For near-UV CD analysis, the mean residue molar ellipticities at 280 nm ($[\theta]_{280}$) were plotted as a function of temperature. (F) For fluorescence spectroscopy, the maximum emission wavelength (λ_{\max}) was plotted as a function of temperature. One of two independent experiments is shown.

FIGURE S4. Partial refolding of CTA1 by sphingomyelin-depleted lipid raft LUVs. Far-UV CD (A) and near-UV CD (B) were used to monitor the structure of CTA1. Measurements of untreated CTA1 were taken at 18°C (solid lines). The toxin was then heated to 37°C and exposed to sphingomyelin-depleted lipid raft LUVs. Additional CD measurements were taken 5 (dotted lines) and 30 (dashed lines) min after a continued 37°C incubation in the presence of LUVs.

FIGURE S5. CTA1 activity in the presence of sphingomyelin-depleted lipid raft LUVs. Two-fold dilutions of CTA1 were mixed with sphingomyelin-depleted lipid raft LUVs at 25°C for toxicity assays performed at 25°C (open squares) or 37°C (closed squares). For a third condition, LUVs were added after the toxin had been heated to 37°C for 30 min (closed triangles). This toxin-LUV mixture was incubated at 37°C for an additional hour before initiating the toxicity assay. Toxin samples incubated in the absence of LUVs at 25°C (open circles) or 37°C (closed circles) were also used for the assay. Four samples were used for each condition; results are presented as means \pm standard errors of the mean.

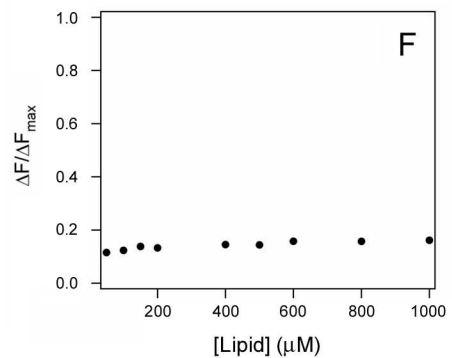
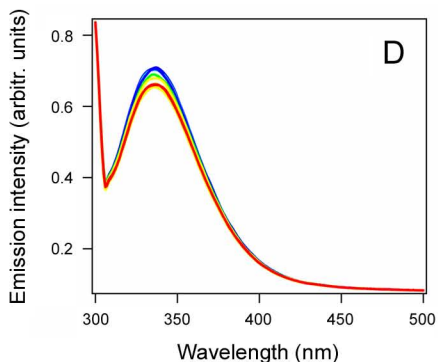
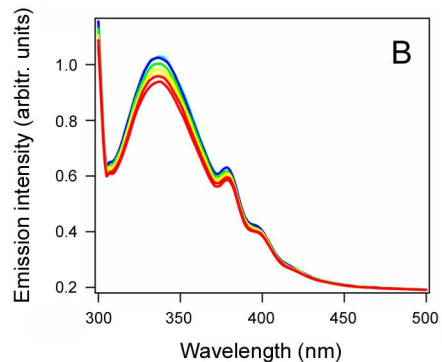
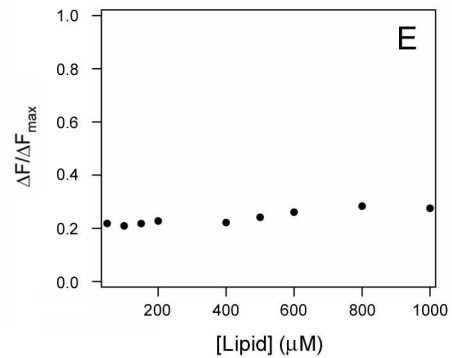
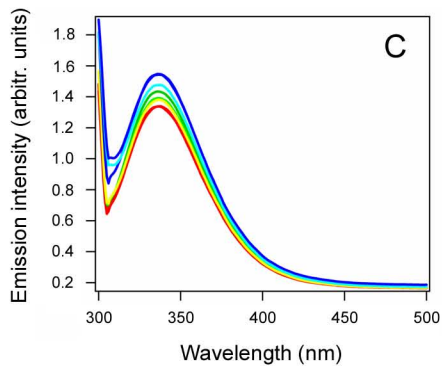
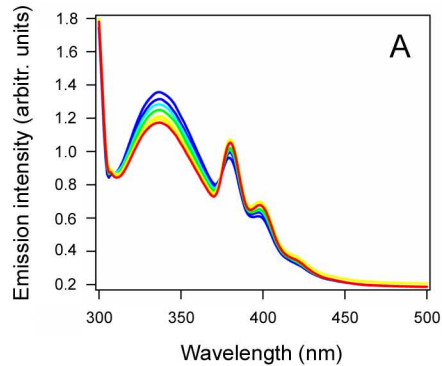


FIGURE S1

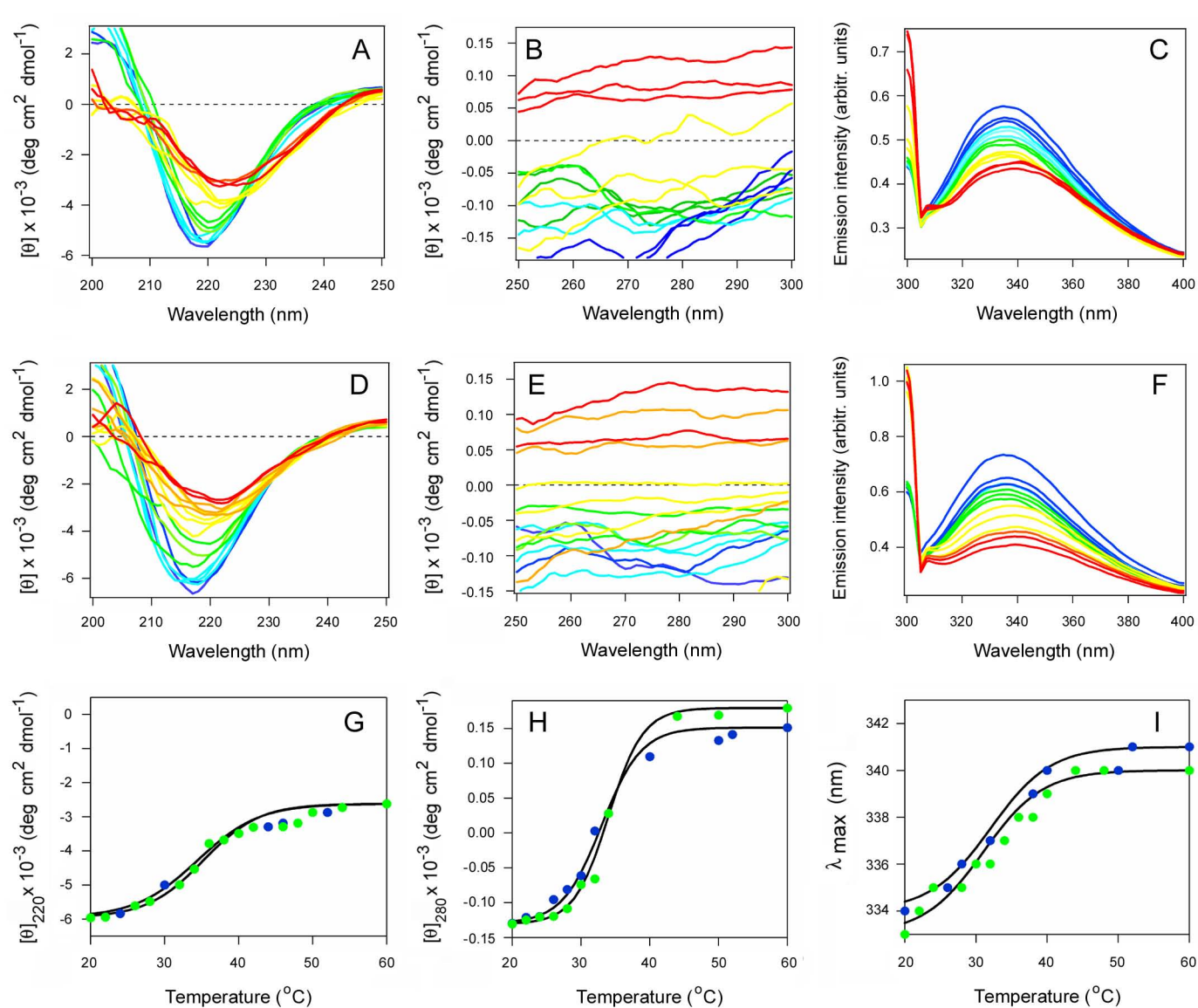


FIGURE S2

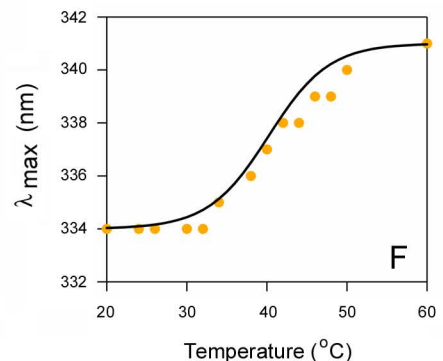
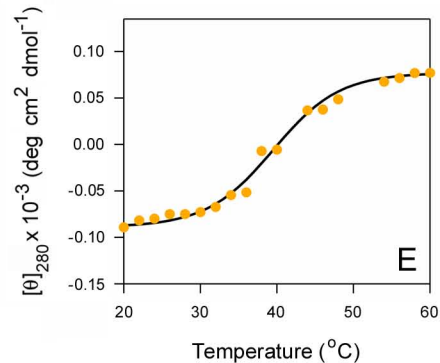
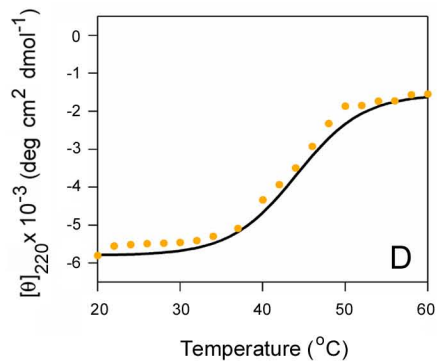
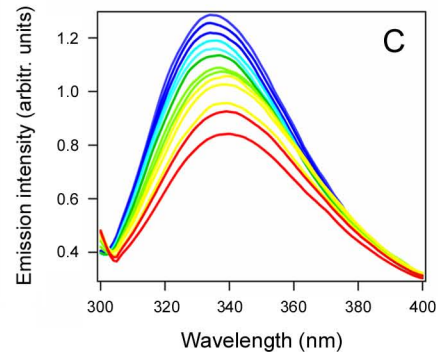
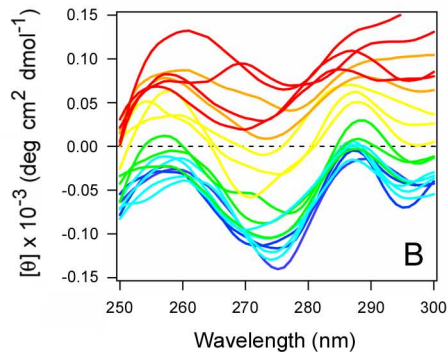
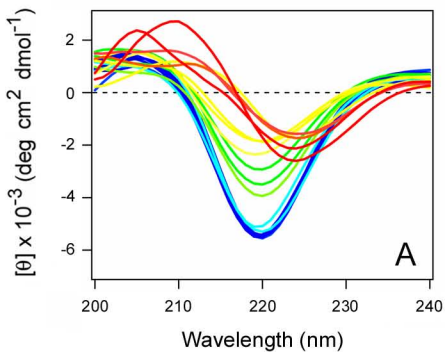


FIGURE S3

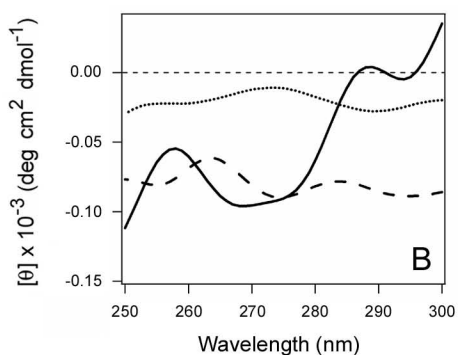
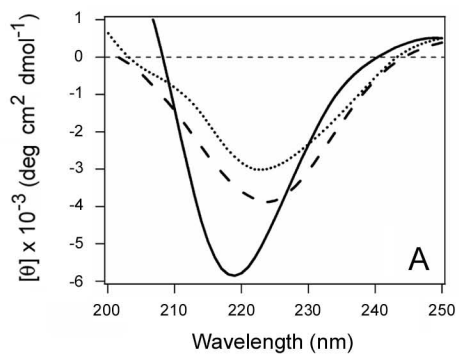


FIGURE S4

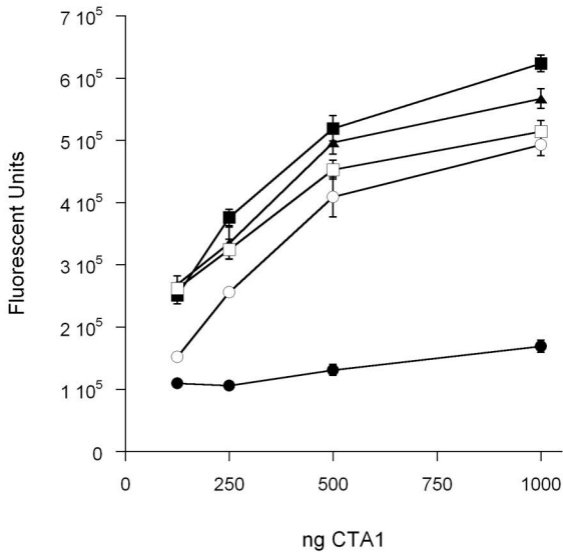


FIGURE S5

Table S1. **CTA1₁₋₁₆₈ stability in the presence of plasma membrane or lipid raft LUVs.**

Toxin condition	T_m (°C)		
	Far-UV CD	Near-UV CD	Fluorescence Spectroscopy
untreated ¹	35	33	35
+ plasma membrane ²	34	33	31
+ lipid raft ²	35	34	32

¹originally reported in Banerjee et. al. (2010) *Biochemistry* **49**(41):8839-8846.

²Calculations were derived from the data presented in Figure S2.